

# Evaluation of AC VRM Topologies for High-Frequency Power Distribution Systems

Laszlo Huber and Milan M. Jovanović

Delta Products Corporation  
Power Electronics Laboratory  
P.O. Box 12173  
5101 Davis Drive  
Research Triangle Park, NC 27709

**Abstract** - In this paper is shown that the regulated series resonant rectifier (SRR) and series-parallel resonant rectifier (SPRR) with variable resonant capacitance are good candidates for ac voltage regulator modules (VRMs) in high-frequency power distribution systems with a sinusoidal ac bus. Control characteristics of the SRR and SPRR are derived using the sinusoidal approximation method. The effect of the transformer magnetizing inductance is also investigated. Experimental results obtained on a 5-V/8.5-A SRR with variable resonant capacitance designed for a 28-V<sub>rms</sub>, 1-MHz sinusoidal ac bus are provided.

## I. INTRODUCTION

Today's high-speed microprocessors represent highly dynamic power loads that necessitate the use of distributed power architectures. Typically, these distributed power-delivery systems use a conventional multiple-output "silver box" as a front end to supply power directly to "not-so-dynamic" loads (e.g., disk drives) and to generate a dc bus for distribution to the dc/dc point-of-load regulators that are used for powering the processors. Generally, these point-of-load regulators, also known as voltage regulator modules (VRMs), are located very close to the processors to minimize the interconnect inductance so that the desired transient response of the VRMs is obtained with a minimal decoupling capacitance [1].

While the described dc-distribution power system has been proven to meet the performance requirements of today's desktop and server power systems, a number of claims have been recently made that a high-frequency ac-distribution power system is a more cost-effective solution to powering today's and future data processing equipment [2], [3], [4]. Generally, these claims are based on the fact that in an ac-distribution power system, which consists of a front-end inverter and ac/dc point-of-load converters (ac VRMs), compared to a dc-distribution power system, two conversion steps (the rectification step in the front-end converter and the inversion step in the point-of-load converter) are eliminated. Because of the reduced number of components, the cost of the ac-distribution power system is expected to be reduced.

The proposals for the high-frequency ac-distribution power systems range from trapezoidal ac-bus systems to pure sinusoidal ac-bus systems with bus frequencies in the MHz range. Generally, it is recognized that the sinusoidal ac-bus system has advantages over the trapezoidal ac-bus system

with respect to EMI performance. However, the sinusoidal ac-bus system requires a more complex inverter and ac VRM design [3]. So far, only one commercial implementation of the ac-distribution power system has been reported [4], which uses 3-5-MHz sinusoidal ac bus. While the size and performance of this ac-distribution power system apparently meet the specifications, the cost-effectiveness of the system is not known.

In this paper, topologies for ac VRMs for HF sinusoidal ac-bus systems are discussed. First, ac VRM topologies are derived from the conventional full-wave rectifier topologies. Next, different control methods for ac VRM output-voltage regulation are evaluated. In Sections III and IV, voltage-transfer-function and input-power-factor characteristics of the proposed ac VRMs are derived and analyzed using the sinusoidal approximation method. The effect of the transformer magnetizing inductance is also investigated. In Section V, a comparison of different ac VRM topologies is given. Experimental results are provided in Section VI.

## II. HF AC VRM TOPOLOGIES

Generally, the conventional full-wave rectifier with voltage-type load (also called peak-detection rectifier), shown in Fig. 1, is not suitable for the HF sinusoidal ac VRMs because of its poor power factor and high current harmonics. The conventional full-wave rectifier with current-type load, shown in Fig. 2, has better power factor than the rectifier with voltage-type load. Ideally, the input current of the circuit in Fig. 2 has rectangular waveform and is in phase with the input voltage, resulting in a theoretical maximum power factor equal to 0.9 [12]. However, because of the circuit parasitics, the achievable power factor is well below 0.9,

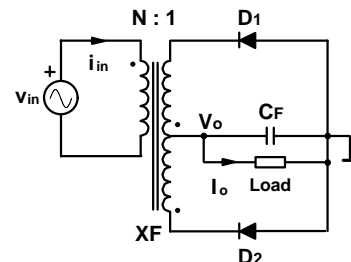


Fig. 1 Conventional full-wave rectifier with voltage-type load

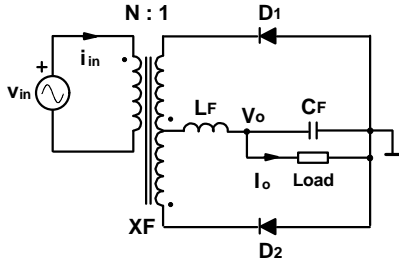


Fig. 2 Conventional full-wave rectifier with current-type load

which is not appropriate for the HF ac power distribution systems.

The input power factor can be significantly improved by adding a series resonant circuit between the ac voltage source and the full-wave rectifier in the circuit in Fig. 1, as shown in Fig. 3, or by adding a series-parallel resonant circuit between the ac voltage source and the full-wave rectifier in the circuit in Fig. 2, as shown in Fig. 4. The circuits in Figs. 3 and 4 are called series resonant rectifier (SRR) and series-parallel resonant rectifier (SPRR), respectively. The SRR with full-wave diode-bridge rectifier, without a transformer, was presented and analyzed in [5] and [6]. A similar analysis of the SPRR was not published yet. Half-wave resonant rectifiers were described in [7].

To obtain close-to-unity power factor, the series resonant circuit in the SRR is tuned near the ac-bus frequency [5], [6]. To achieve output-voltage regulation with the SRR, three control approaches can be used [8]: (1) SRR with variable resonant inductance, (2) SRR with variable resonant capacitance, and (3) SRR with constant resonant frequency by controlling the phase-angle of the rectified current. Generally, the SRR control methods (1) and (3) are less attractive than control method (2). Namely, a variable inductance can be implemented by changing the effective permeability of the core [8], [9] or by switching the inductor current, which requires a bidirectional switch connected in series with the inductor [10]. For the first implementation of the variable inductance, it is hard to control the output voltage in a wide load range [9]; whereas, for the second implementation the full input current flows through two switches connected in series [10]. The phase-angle control method can be implemented by connecting a bidirectional switch in parallel to the input of the full-wave rectifier [8],

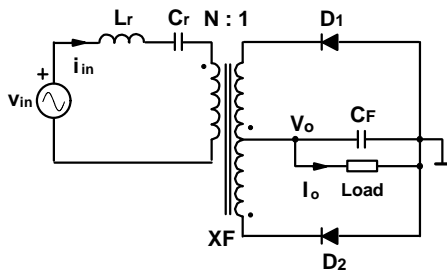


Fig. 3 Series resonant rectifier

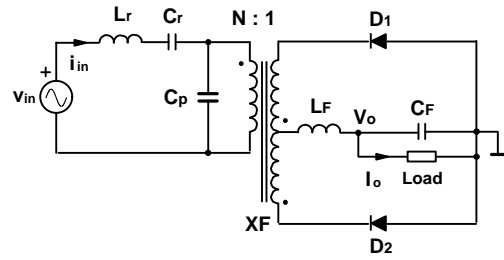


Fig. 4 Series-parallel resonant rectifier

[11]. If the ac VRM contains a transformer, the bidirectional switch can be connected in parallel either with the primary or secondary winding of the transformer [8]. However, the phase-angle-control switches operate with hard switching, making the phase-angle control not very suitable for the HF ac VRMs. A variable capacitance can be implemented with a switch-controlled capacitor, which requires a bidirectional switch connected in parallel with the capacitor [10]. The operation of the switch-controlled capacitor is very efficient because the switches operate with zero voltage switching (ZVS) and they carry only a small portion of the input current. Therefore, the regulated SRR with variable resonant capacitance is a good candidate for the HF sinusoidal ac VRMs especially for wide load ranges. The same conclusions can be extended to the SPRRs.

### III. SRR WITH VARIABLE CAPACITANCE

Control characteristics of the regulated SRR with variable resonant capacitance can be obtained using the sinusoidal (fundamental) approximation method [12], which simplifies the SRR to the circuit shown in Fig. 5, where  $L_m$  is the magnetizing inductance of the transformer. In Fig. 5, it is assumed that the leakage inductance of the transformer is lumped with the resonant inductance  $L_r$ . If the ac-bus voltage is defined as

$$v_{in} = V_{in,pk} \cdot \sin(\omega_n t) \quad , \quad (1)$$

then, the voltage transfer function is

$$M = \frac{NV_o}{V_{in,pk}} = \frac{\pi}{4} \cdot \frac{1}{\sqrt{\left(1 + k_{Lm} (1 - \omega_n^2)\right)^2 + Q_{eq}^2 (1 - \omega_n^2)^2}} \quad , \quad (2)$$

where  $\omega_n$  is the resonant frequency of the series resonant circuit,

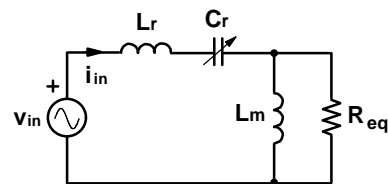


Fig. 5 Equivalent circuit of SRR with variable resonant capacitance

$$\omega_r = \frac{1}{\sqrt{L_r C_r}}, \quad (3)$$

normalized to the input frequency, i.e.,

$$\omega_n = \frac{\omega_r}{\omega_{in}}; \quad (4)$$

$Q_{eq}$  is the equivalent quality factor defined as

$$Q_{eq} = \frac{\omega_{in} L_r}{R_{eq}}, \quad (5)$$

where  $R_{eq}$  is the equivalent load resistance,

$$R_{eq} = \frac{8}{\pi^2} \cdot N^2 R_{load}; \quad (6)$$

and  $k_{Lm}$  is the magnetizing-inductance factor, defined as the reciprocal value of the magnetizing inductance normalized to the resonant inductance, i.e.,

$$k_{Lm} = \frac{L_r}{L_m}. \quad (7)$$

It should be noted that the equivalent quality factor in (5) can also be interpreted as the reciprocal value of the normalized

equivalent load resistance. Similarly, from Fig. 5, the input power factor can be obtained as

$$PF = \frac{1}{\sqrt{\left[ \left( 1 + k_{Lm} (1 - \omega_n^2) \right)^2 + Q_{eq}^2 (1 - \omega_n^2)^2 \right]} \cdot \left( 1 + \frac{k_{Lm}^2}{Q_{eq}^2} \right)}. \quad (8)$$

For an ideal transformer  $k_{Lm} = 0$ , the voltage-transfer-function and input-power-factor characteristics versus normalized resonant frequency  $\omega_n$  and quality factor  $Q_{eq}$  as parameter are shown in Fig. 6. It should be noted that  $Q_{eq} = \pi/4$  is the minimum value of  $Q_{eq}$  required for the rectifier to operate in continuous conduction mode [5], [6]. As can be seen from Fig. 6, at  $\omega_n = 1$ , the voltage conversion ratio does not change with the load variations and the power factor is unity. Therefore, the SRR ideally meets the ac VRM requirements. However, because of the parasitic series resistances in a practical circuit, the voltage conversion ratio of the SRR varies with the load variation even if the series resonant circuit (including the series parasitic inductances) is ideally tuned to the input frequency. It can be also seen from Fig. 6 that if the series resonant circuit is detuned from the input frequency, both the voltage conversion ratio and the

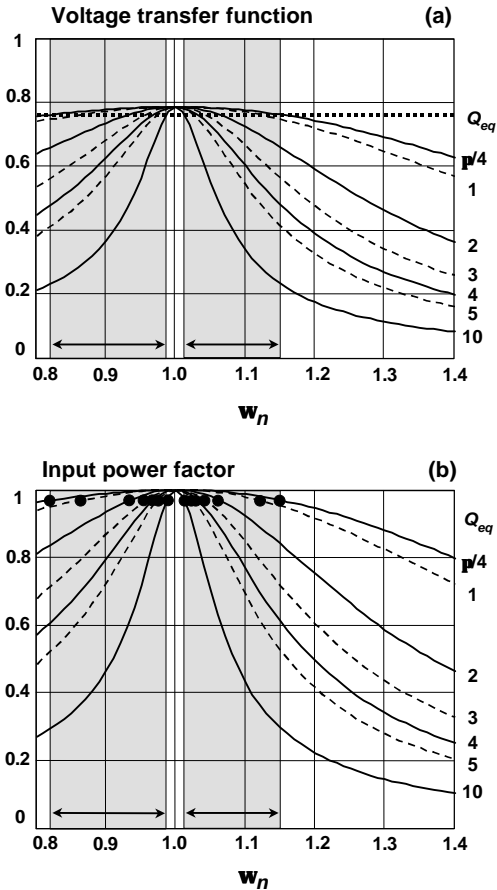


Fig. 6 Control characteristics of SRR with ideal transformer

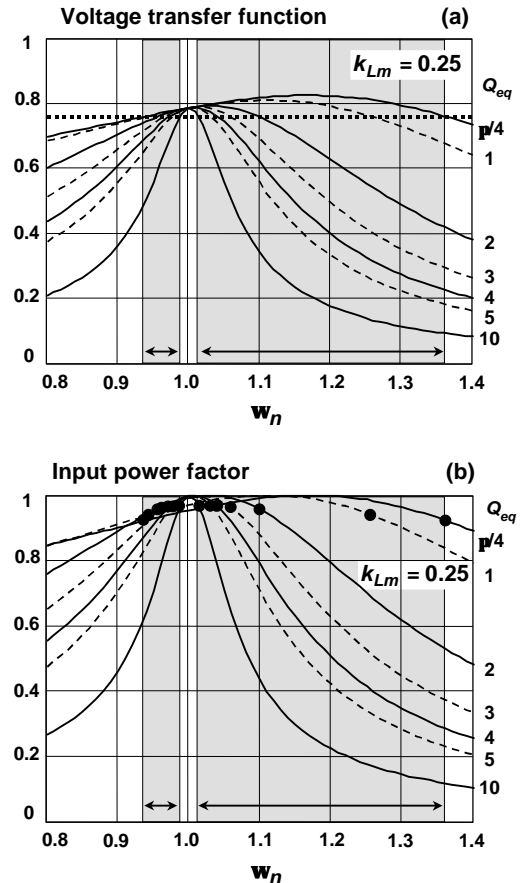


Fig. 7 Control characteristics of SRR with non-ideal transformer

power factor decrease with increasing load current. Finally, it can be seen from Fig. 6 that to regulate the output voltage against load variations (horizontal dotted line in Fig. 6), for the same load range, the operation above the input frequency,  $\omega_n > 1$ , requires a slightly smaller variation of the resonant frequency than the operation below the input frequency,  $\omega_n < 1$ , whereas, the power factor is maintained constant.

Taking into account the magnetizing inductance of the transformer, for a typical value of  $k_{Lm}$  ( $k_{Lm} = 0.25$ ), the voltage-transfer-function and input-power-factor characteristics versus  $\omega_n$  and  $Q_{eq}$  as parameter are presented in Fig. 7. As can be seen from Fig. 7, as  $Q_{eq}$  decreases, the voltage-transfer-function curves are shifted to the right with an increased peaking compared to the corresponding curves in Fig. 6. All curves pass through the point ( $\omega_n = 1, M = \pi/4$ ). Similarly, the power factor curves are also shifted to the right with decreasing  $Q_{eq}$ . The shifting of the resonant characteristics can be easily explained by converting the parallel  $L_m$ - $R_{eq}$  circuit in Fig. 5 into a series  $L_{m,ser}$ - $R_{eq,ser}$  circuit. Due to the additional series inductance,  $L_{m,ser}$ , to achieve resonance at the input frequency, capacitance  $C_r$  needs to be decreased, and, therefore, the resonant frequency of the series resonant circuit  $L_r$ - $C_r$ ,  $\omega_r = 1/\sqrt{L_r C_r}$  increases, resulting in shifting of the resonant characteristics to the right. At resonance, the normalized resonant frequency of the series resonant circuit  $L_r$ - $C_r$  is equal to

$$\omega_{n,res} = \sqrt{1 + \frac{1}{k_{Lm}} \cdot \frac{1}{1 + \left(\frac{Q_{eq}}{k_{Lm}}\right)^2}}, \quad (9)$$

and the peak value of the voltage conversion ratio is determined as

$$M_{pk} = \frac{\pi}{4} \cdot \sqrt{1 + \left(\frac{k_{Lm}}{Q_{eq}}\right)^2}. \quad (10)$$

It follows from (9) and (10) that with decreasing  $Q_{eq}$ , both the normalized resonant frequency  $\omega_{n,res}$  and the peak value of the voltage conversion ratio  $M_{pk}$  increase.

As can be seen from Fig. 7 (horizontal dotted line), to regulate the output voltage in the same load range, assuming a constant input voltage, the required variation of the resonant frequency is significantly smaller if the resonant frequency of the series  $L_r$ - $C_r$  circuit is below the input frequency, i.e.,  $\omega_n < 1$ , compared to  $\omega_n > 1$ . At the same time, the input power factor maintains the same value for the same load below and above  $\omega_n = 1$ . It can be concluded from Fig. 7 that the preferred area of operation is  $\omega_n < 1$ . Therefore, the variable resonant capacitance should be designed to increase as the load decreases. The switch-controlled capacitor [10] satisfies this criteria, i.e., at the maximum load, the capacitance is minimal and equal to its nominal value,

whereas, with a decreasing load, the capacitance effectively increases.

#### IV. SPRR WITH VARIABLE CAPACITANCE

Applying the sinusoidal (fundamental) approximation method [12] to the SPRR in Fig. 4, the equivalent circuit shown in Fig. 8 is obtained, where the equivalent load resistance is defined as

$$R_{eq} = \frac{\pi^2}{8} \cdot N^2 R_{load}. \quad (11)$$

If it is assumed that the transformer is ideal, the voltage transfer function can be expressed as

$$M = \frac{NV_o}{V_{in,pk}} = \frac{2}{\pi} \cdot \frac{1}{\sqrt{\left(1 - C_n(1 - \omega_n^2)\right)^2 + Q_{eq}^2(1 - \omega_n^2)^2}}, \quad (12)$$

where  $\omega_n$  is the normalized resonant frequency of the series resonant circuit  $L_r$ - $C_r$ , defined as in (3) and (4);  $Q_{eq}$  is the equivalent quality factor, defined as in (5); and  $C_n$  is the normalized parallel capacitance defined as

$$C_n = \frac{C_p}{C_{r0}}, \quad (13)$$

where  $C_{r0}$  is the capacitance of the series capacitor  $C_r$  when  $C_r$  resonates with  $L_r$  at the input frequency,

$$\omega_{in} = 1/\sqrt{L_r C_{r0}}. \quad (14)$$

Also from Fig. 8, the input power factor is obtained as

$$PF = \frac{1}{\sqrt{1 + \left[Q_{eq}(1 - \omega_n^2) + \frac{C_n}{Q_{eq}}(C_n(1 - \omega_n^2) - 1)\right]^2}}. \quad (15)$$

For a reasonable value of  $C_n$  ( $C_n = 0.25$ ), the voltage-transfer-function and input-power-factor characteristics versus  $\omega_n$  and  $Q_{eq}$  as parameter are presented in Fig. 9. As can be seen from Fig. 9, as  $Q_{eq}$  decreases, the voltage-transfer-function curves are shifted to the left with an increased peaking compared to the corresponding curves in Fig. 6 ( $C_n = 0$ ). All curves pass through the point ( $\omega_n = 1, M = 2/\pi$ ). Similarly, the power-factor curves are also shifted to the left with decreasing  $Q_{eq}$ . The shifting of the resonant characteristics can be explained, similarly as in Section III, by converting the parallel  $C_p$ - $R_{eq}$  circuit into a series  $C_{p,ser}$ -

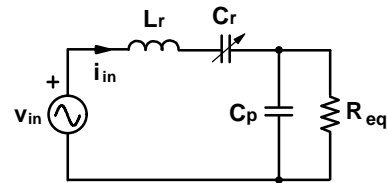


Fig.8 Equivalent circuit of SPRR with variable resonant capacitance

$R_{eq,ser}$  circuit. Due to the additional series capacitance,  $C_{p,ser}$ , to achieve resonance at the input frequency, capacitance  $C_r$  needs to be increased, and, therefore, the resonant frequency of the series resonant circuit  $L_r-C_r$ ,  $\omega_r = 1/\sqrt{L_r C_r}$  decreases, resulting in shifting of the resonant characteristics to the left. At resonance, the normalized resonant frequency of the series resonant circuit  $L_r-C_r$  is equal to

$$\omega_{n,res} = \sqrt{1 - \frac{1}{C_n} \cdot \frac{1}{1 + \left(\frac{Q_{eq}}{C_n}\right)^2}} \quad (16)$$

and the peak value of the voltage conversion ratio is determined as

$$M_{pk} = \frac{2}{\pi} \cdot \sqrt{1 + \left(\frac{C_n}{Q_{eq}}\right)^2} \quad (17)$$

It follows from (16) and (17) that with decreasing  $Q_{eq}$ , the normalized resonant frequency  $\omega_{n,res}$  decreases while the peak value of the voltage conversion ratio  $M_{pk}$  increases.

As can be seen from Fig. 9 (horizontal dotted line), to

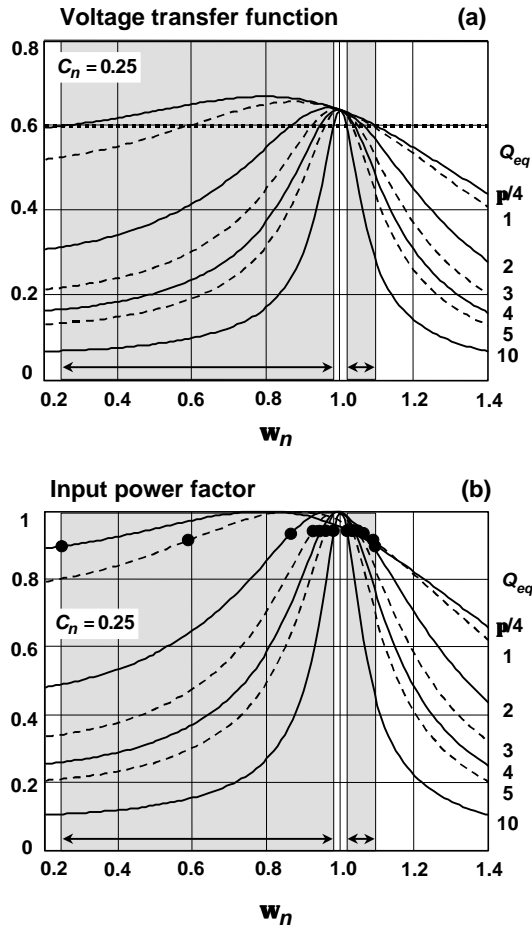


Fig. 9 Control characteristics of SPRR with ideal transformer

regulate the output voltage in the same load range, assuming a constant input voltage, the required variation of the resonant frequency is significantly smaller if the resonant frequency of the series  $L_r-C_r$  circuit is above the input frequency, i.e.,  $\omega_n > 1$ , compared to  $\omega_n < 1$ . At the same time, the input power factor maintains the same value for the same load above and below  $\omega_n = 1$ . It can be concluded from Fig. 9 that the preferred area of operation is  $\omega_n > 1$ , which is opposite to the preferred area of operation of the SRR.

When the magnetizing inductance of the transformer is taken into account, a parallel resonant circuit is formed in parallel with the equivalent load resistance  $R_{eq}$  in Fig. 8. The resonant frequency of the parallel  $L_m-C_p$  circuit is defined as

$$\omega_p = \frac{1}{\sqrt{L_m C_p}} \quad (18)$$

If  $\omega_p > \omega_m$ , the parallel  $L_m-C_p$  circuit has inductive nature and the SPRR shows similar characteristics to the SRR with  $L_m$ , (Fig. 7). If  $\omega_p < \omega_m$ , the parallel  $L_m-C_p$  circuit has capacitive nature and the SPRR has similar characteristics as shown in Fig. 9. Finally, if  $\omega_p = \omega_m$ , the characteristics of the SPRR are similar to the characteristics of the SRR with an ideal transformer, shown in Fig. 6. Therefore, the SPRR with a parallel resonant circuit tuned to the input frequency has the potential to closely meet the ac-VRM requirements.

The SPRR in Fig. 4 is implemented with a full-wave rectifier with center-tapped transformer (CTXF). Another possible implementation of the SPRR is with a current-doubler rectifier (CDR) as shown in Fig. 10. The equivalent circuit of the SPRR with CDR is identical to the circuit in Fig. 8. The only difference is in the value of the equivalent load resistance, which is for the SPRR with CDR determined as

$$R_{eq} = \frac{\pi^2}{2} \cdot N^2 R_{load} \quad (19)$$

The voltage-transfer-function and input-power-factor characteristics of the SPRR with CDR comply with expressions (12) and (15), respectively. The only difference is in the value of the multiplication factor in (12), which is equal to  $1/\pi$  instead of  $2/\pi$ .

It should be noted that the efficiency of the ac VRMs can be improved by replacing the rectifier diodes in Figs. 3, 4, and 10 with synchronous rectifiers (SRs).

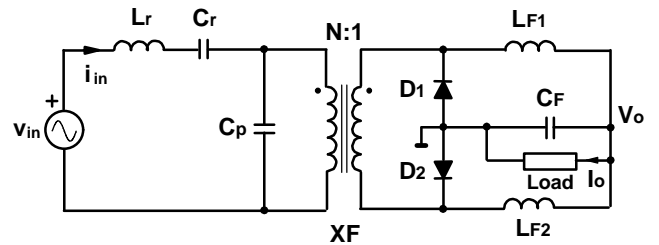


Fig. 10 SPRR with current doubler rectifier

## V. COMPARISON OF AC VRM TOPOLOGIES

A comparison of the proposed resonant rectifier topologies for ac VRMs is presented in Table I. Table I lists the normalized turns ratio of the transformer, the normalized rms currents of the transformer primary and secondary windings, and the normalized current and voltage stresses of the synchronous rectifiers. For simplicity, it was assumed that all components are ideal. As can be seen from Table I, the SPRR with CDR has the smallest current stress in the secondary winding, while the SRR has the smallest current stress in the primary winding. The synchronous rectifiers in the SPRR have smaller current stress but larger voltage stress than in the SRR.

TABLE I  
COMPARISON OF AC VRM TOPOLOGIES

	SRR	SPRR	
		CTXF	CDR
$N / (V_{in,pk} / V_o)$	0.785	0.637	0.318
$I_{prim,rms} / (I_o \cdot (V_o / V_{in,pk}))$	1.41	1.57	1.57
$I_{sec,rms} \text{ (winding)} / I_o$	0.785	0.707	0.5
$I_{sec,rms} \text{ (total)} / I_o$	1.11	1	0.5
$I_{SR,rms} / I_o$	0.785	0.707	0.707
$V_{SR} / V_o$	2	3.14	3.14

## VI. EXPERIMENTAL RESULTS

The feasibility of resonant rectifiers for ac VRMs is illustrated on a regulated SRR with variable resonant capacitance. The experimental 5-V/8.5-A ac VRM was designed for a 28-V<sub>rms</sub>, 1-MHz sinusoidal ac bus. The circuit diagram of the experimental ac VRM is shown in Fig. 11. The transformer and the resonant inductor are implemented by using planar cores E/PLT 18/4/10. All the MOSFETs operate without heatsinks. Experimental waveforms of the input voltage, input current, and resonant-capacitor voltage at 100%, 50%, and 10% loads are presented in Fig. 12. As can be seen from Fig. 12, at 100% and 50% loads, the input current is sinusoidal with a small phase delay compared to the input voltage. However, at 10% load, the input current is more distorted because of the superimposed magnetizing

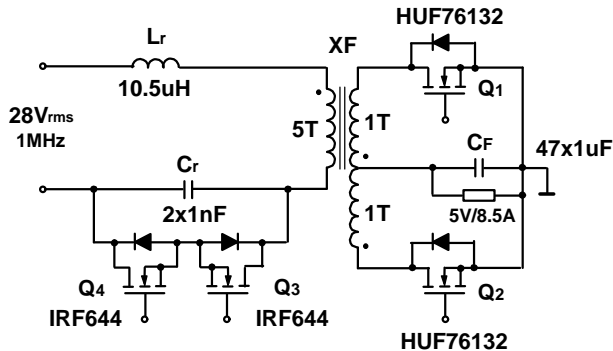


Fig. 11 Experimental ac VRM

current which cannot be neglected at light loads. Temperature measurements obtained at full load, without forced cooling are presented in Table II.

TABLE II  
MEASURED TEMPERATURES AT 100% LOAD  
WITHOUT FORCED COOLING ( $T_{amb} = 23^\circ\text{C}$ )

$T(L_r\text{-}Fe)$ [°C]	$T(L_r\text{-}Cu)$ [°C]	$T(XF\text{-}Fe)$ [°C]	$T(XF\text{-}Cu)$ [°C]	$T(Q_1)$ [°C]	$T(Q_2)$ [°C]
58	60	41	44	42	38

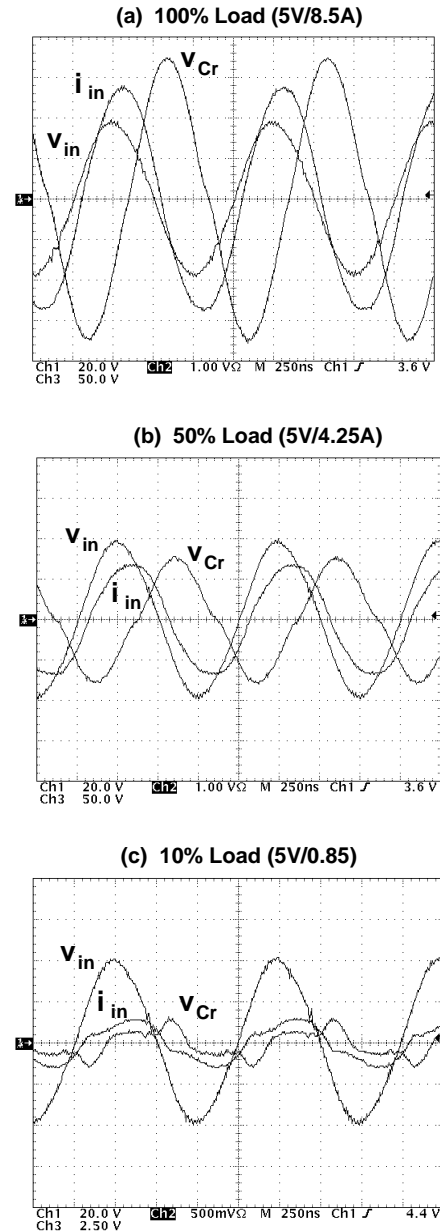


Fig. 12 Experimental waveforms of input voltage, input current, and resonant-capacitor voltage at (a) 100%, (b) 50%, and (c) 10% load

## VII. SUMMARY

In this paper, an evaluation of the resonant rectifiers for ac VRMs in HF power distribution systems with a sinusoidal ac bus is performed. Three resonant rectifier topologies are investigated: the series resonant rectifier (SRR), the series-parallel resonant rectifier (SPRR) with center-tapped transformer, and the SPRR with current doubler rectifier (CDR). The control characteristics of the ac VRMs are derived and analyzed using the sinusoidal approximation method.

It is shown that the power factor of the SRR is reduced at very light loads because of the magnetizing current of the transformer. This problem is less pronounced with the SPRR, because the effect of the transformer's magnetizing inductance can be compensated by the parallel capacitance of the SPRR. At larger load currents, the SPRR with CDR is the preferred topology because of the significantly reduced current stress in the transformer's secondary winding. Experimental results obtained on a 5-V/8.5-A SRR with variable resonant capacitance designed for a 28-V<sub>rms</sub>, 1-MHz sinusoidal ac bus are provided.

## REFERENCES

- [1] M.T. Zhang, M.M. Jovanoviæ, and F.C. Lee, "Design considerations for low-voltage on-board dc/dc modules for next generations of data processing circuits," *IEEE Trans. on Power Electronics*, vol. 11, no. 2, pp. 328-337, Mar. 1996.
- [2] J. Drobnik, L. Huang, P. Jain, and R. Steigerwald, "PC platform power distribution system: past application, today's challenge and future direction," *IEEE International Telecommunications Energy Conf. (INTELEC) Proc.*, paper no. 2-1, Jun. 1999.
- [3] A. Gentchev and D.P. Arduini, "An ac high frequency quasi square wave bus voltage for the next generation of distributed power systems," *High frequency Power Conversion (HFPC) Proc.*, pp. 89-103, Oct. 1998.
- [4] B. Porter, "High frequency conversion for powering microprocessors," *HP GPST Power Supply Technology Symposium Proc.*, Oct. 2000.
- [5] V. Vorperian and R.B. Ridley, "A simple scheme for unity power-factor rectification for high frequency ac buses," *IEEE Trans. Power Electronics*, vol. 5, no. 1, pp. 77-87, Jan. 1990.
- [6] S. Freeland, "Input current shaped ac-to-dc converters," NASA Report, NASA-CR-176787, May 1986.
- [7] W.A. Nitz, W.C. Bowman, F.T. Dickens, F.M. Magalhaes, W. Strauss, W.B. Suiter, and N.G. Ziesse, "A new family of resonant rectifier circuits for high frequency dc-dc converter applications," *IEEE Applied Power Electronics Conf. (APEC) Proc.*, pp. 12-22, Feb. 1988.
- [8] W. Chen, R. Watson, G. Hua, and F.C. Lee, "Development of a regulated resonant rectifier for ac-distributed systems," *VPEC Seminar Proc.*, pp. 259-265, Sep. 1994.
- [9] C. Leu, M. Tullis, L. Keller, and F.C. Lee, "A high-frequency ac bus distributed power system," *VPEC Seminar Proc.*, pp. 98-107, Sep. 1990.
- [10] K. Harada, W.J. Gu, and K. Murata, "Controlled resonant converters with switching frequency fixed," *IEEE Power Electronics Specialists Conf. (PESC) Rec.*, pp. 431-438, Jun. 1987.
- [11] M.C. Tanju and K. Jain, "High-performance ac/dc converter for high-frequency power distribution systems: analysis, design considerations, and experimental results," *IEEE Power Electronics Specialists Conf. (PESC) Rec.*, pp. 1156-1162, Jun. 1992.
- [12] R. Erickson, *Fundamentals of Power Electronics*, New York, NY: Chapman&Hall, 1997.